Open Veterinary Journal, (2024), Vol. 14(10): 2662-2677
ISSN: 2226-4485 (Print)
ISSN: 2218-6050 (Online)
Research Article
DOI: *10.5455/OVJ.2024.v14.i10.16*

Submitted: 05/08/2024 Accepted: 08/09/2024 Published: 31/10/2024

Effect of Java plum (*Syzygium cumini*) leave extract and a silver nanoparticles synthesis on pathogens in skin diseases of dogs

Namthip Wongstitwilairoong[1], Usuma Jermnark[1], Napasorn Paochoosak[1], Orawan Limsivilai[2], Wissanuwat Chimnoi[3], Yared Beyene Yohannes[4], Yoshinori Ikenaka[4,5,6,7] and Aksorn Saengtienchai[1]*

[1]*Department of Pharmacology, Faculty of Veterinary Medicine, Kasetsart University, Bangkok, Thailand*
[2]*Department of Microbiology and Immunology, Faculty of Veterinary Medicine, Kasetsart University, Bangkok, Thailand*
[3]*Department of Parasitology, Faculty of Veterinary Medicine, Kasetsart University, Bangkok, Thailand*
[4]*Laboratory of Toxicology, Department of Environmental Veterinary Science, Faculty of Veterinary Medicine, Hokkaido University, Sapporo, Japan*
[5]*Veterinary Teaching Hospital, Graduate School of Veterinary Medicine, Hokkaido University, Sapporo, Japan*
[6]*One Health Research Center, Hokkaido University, Sapporo, Japan*
[7]*Water Research Group, Unit for Environmental Science and Management, North-West University, Potchefstroom, South Africa*

Abstract

Background: Antibiotic use has been rising in both humans and animals. The growing concern over antimicrobial drug resistance and the promotion of regional drug use have led to a rise in the interest in medicinal applications of herbs combined with biosynthesized nanoparticles.

Aim: To evaluate the antimicrobial and acaricidal effects of *Syzygium cumini* leaves crude extract (Sc-CE) and biosynthesized *S. cumini* silver nanoparticles (Sc-AgNPs) on dog skin pathogens and determined the optimal concentration and time for *in vitro* application.

Methods: *Syzygium cumini* leaves (Sc) were prepared as Sc-CE and Sc-AgNPs. The biosynthesized silver nanoparticles were characterized employing various techniques, including dynamic light scattering, scanning electron microscopy, and energy-dispersive X-ray analysis. Phytochemical analyses were conducted using liquid chromatography coupled with quadrupole time-of-flight mass spectrometry screening. Antimicrobial activity was examined against gram-positive bacteria, including *Staphylococcus aureus* and *Staphylococcus pseudintermedius*, gram-negative bacteria such as *Pseudomonas aeruginosa*, yeast strains including *Malassezia pachydermatis* and *Candida albicans*, and ectoparasite. Cytotoxicity was evaluated on canine primary dermal fibroblast (CPDF) using the 3-(4,5-dimethylthiazol-2-yl)-2,5-diphenyltetrazolium bromide assay.

Results: The Sc-AgNPs exhibited nanoparticle sizes ranging from 100 to 350 nm with aggregated spherical shape and contained Ag element in this nanoparticle. Myricetin and Phloretin were among the extracted compounds, contributing to the reduction of pathogenic organisms. Sc-AgNPs showed high efficacy against skin pathogens compared to Sc-CE, with a lower cytotoxicity effect on CPDF.

Conclusion: The Sc-AgNPs demonstrated superior efficiency against pathogens in dog skin diseases as both concentration- and time-dependent and were deemed safe to CPDF within 24 hours.

Keywords: Acaricidal activity, Antimicrobial activity, Green synthesis, Silver nanoparticles, *Syzygium cumini.*

Introduction

Antimicrobial resistance refers to the capacity of microorganisms to endure the presence of antimicrobial substances. This issue is of primary concern to clinicians and highlights a critical threat to public health, making it a top global priority in healthcare (WHO, 2017). The prevalence of resistant bacterial strains and antibiotic resistance-related mortality is a global concern, including in Thailand (Kaneria and Chanda, 2013). Consequently, extensive research has been granted to explore alternative approaches for addressing diseases caused by microorganisms with the aim of reducing the tendency toward unnecessary antibiotic overuse. A focal point of this evaluation involves investigating the potential of natural products, specifically medicinal plants, as alternatives to antibiotics. Beyond their

***Corresponding Author:** Aksorn Saengtienchai. Department of Pharmacology, Faculty of Veterinary Medicine, Kasetsart University, Bangkok, Thailand. Email: *fvetasc@ku.ac.th*

recognized antimicrobial capabilities, these plants have been shown in studies to have anti-inflammatory, analgesic, and antioxidant effects, providing a wide range of therapeutic benefits for both humans and animals.

Syzygium cumini (L.) (Sc) (synonyms: *Eugenia jambolana*, *Syzygium jambolana*, *Eugenia cumini*), commonly known as Jamun, Jambul, Jambolao, Java plum, Indian blackberry, and black plum, belongs to the family Myrtaceae (Singh and Navneet, 2021). Sc has been traditionally used as a medicinal plant. Different parts of the plant (bark, leaves, seeds, and fruit) have been employed in treating various diseases such as diabetes and dysentery, in reducing jaundice, and as an antidote for opium poisoning (Biologicals, 2014; CLSL, 2020; Hemlata *et al.*, 2020).

Traditionally, *S. cumini* has been documented for its efficacy in addressing a spectrum of health conditions. Furthermore, the solution of *Syzygium cumini* leaves crude extract (Sc-CE) has demonstrated notable therapeutic properties, encompassing antimicrobial, anti-inflammatory, anti-nociceptive, antioxidant, antihyperlipidemic, and cardioprotective attributes (Citron *et al.*, 1991; Barry *et al.*, 1999; Arikan, 2007; Balouiri *et al.*, 2016; Bubonja-Šonje *et al.*, 2020).

Jambolan boasts a wealth of compounds, including anthocyanins, glucoside, ellagic acid, isoquercetin, kaempferol, and myricetin. The seeds are reputed to harbour alkaloid jambosine and glycoside jambolin, also known as antimellin. This combination is purported to impede the diastatic conversion of starch into sugar (Konaté *et al.*, 2012). The leaves are rich in acylated flavonol glycosides, quercetin, myricetin, myricetin, myricetin 3-O-4-acetyl-L-rhamnopyranoside, triterpenoid, esterase, galloyl carboxylase, and tannin (CLSL, 2020).

Nanobiotechnology represents the integration of nanotechnology into the realm of biological sciences. A major focus within this field involves the synthesis of nanoparticles, a process leveraging substances with diverse chemical compositions, sizes, shapes, and molecular distributions. This synthesis process has been refined to prioritize cleanliness, non-toxicity, and environmental friendliness. It encompasses three primary methods; (1) Physical Method: This involves nanoparticle synthesis through processes such as evaporation-condensation and laser ablation (2) Chemical Method: This category includes the use of both organic and inorganic substances as reducing agents, as well as employing electrochemical techniques, physicochemical reduction techniques, and microwave-assisted synthesis, and (3) Biological Method: Utilizing living organisms such as bacteria, fungi, algae, or plants for nanoparticle synthesis is a widely adopted approach. The resulting nanoparticles exhibit high stability and possess unique properties contingent on the specific biological entities employed in the synthesis (Pfaller *et al.*, 2004; Weber *et al.*, 2019).

This research aims to investigate the impact of Sc-CE and *S. cumini* silver nanoparticles (Sc-AgNPs) on microorganisms and ectoparasites responsible for causing skin diseases in dogs and cytotoxicity to canine primary dermal fibroblast (CPDF) and to establish a comprehensive biological activity index by assessing the combined efficacy of nanoparticles.

Materials and Methods

Chemicals

The 24-well macro dilution plate (Thermo Fisher Scientific, UK), Cell Proliferation Kit I **3**-(4,5-dimethylthiazol-2-yl)-2,5-diphenyltetrazolium bromide (MTT) (REF: 11465007001) (Roche, Indiana, USA), Dimethyl sulfoxide (DMSO) (Thermo Fisher Scientific, UK), Distilled water, Dulbecco's Modified Eagle Medium (DMEM) (Thermo Fisher Scientific, UK), Fetal Bovine Serum (FBS) (Thermo Fisher Scientific, UK), Flat bottom 96 well cell culture plate (Corning Costar, USA), Methanol A.R. grade (RCI Labscan, Thailand), Mueller Hilton Agar (MHA) (Becton Dickinson and Company, USA), Phosphate Buffe Saline, RPMI 1640 (Thermo Fisher Scientific, UK), Sabouraud Dextrose Agar (Becton Dickinson and Company, USA), Sabouraud Dextrose Broth (Becton Dickinson and Company, USA), Silver nitrate ($AgNO_3$) A.R. grade (Qrec, New Zealand), T75 Tissue Culture Flask (Thermo Fisher Scientific, UK), Tryptiase Soy Broth (Becton Dickinson and Company, USA), Tween 80 (Krungthepchemi, Thailand), and all other chemicals and agents used were an analytical grade and high purity.

Collection of plant materials and preparation of extracts

Fresh leaves of Sc were collected from the local area of Ang Thong province, Thailand. A voucher number of specimen (TTM No.0006796) was deposited at the Herbarium of Thai Traditional Medicine Research Institute, Bangkok, Thailand. The fresh leaves were cleaned with distilled water, sliced, dried in a drying oven at 60°C (Memmert, Germany), and then ground into powder form. One hundredth gram of powdered leaves of Sc were sequentially extracted with 1 l of 100% methanol in a light-protected bottle for 24 hours at 4°C. Then samples were sonicated using Probe Sonicator UW 2200 with Sonoplus 497 Titanteller TT 13 (Bandelin, Germany) for 20 minutes and centrifuged with High-Speed Refrigerated Centrifuge 5810R (Eppendorf, Germany) at 3,200 rpm for 15 minutes. The supernatant was filtered through Whatman No.2 filter paper and evaporated to dryness under reduced pressure at 40°C by Rotavapor R300 (Buchi, Flawil, Switzerland). The Sc-CE was dissolved in 100 mg/ml DMSO, which was diluted to 0.1% (*v*/*v*) for antimicrobial activities in a culture medium. Then Sc-CE solution was kept at 4°C until used (Kaneria and Chanda, 2013).

Phytochemical analysis

The phytochemical analysis was performed in the Laboratory of Toxicology, Faculty of Veterinary Medicine, Hokkaido University, Japan. Five milligrams of Sc-CE were prepared in methanol to achieve a final concentration of 0.25 mg/ml. Phytochemical compounds in the Sc-CE were identified using Agilent 6546 liquid chromatography coupled with quadrupole time-of-flight mass spectrometry screening (LC/QTOF-MS) (Agilent, USA). The LC system was equipped with a Poroshell 120, EC-C18 (2.7 µm, 3.0 × 150 mm) column (Agilent). The mobile phase consisted of 2 mM ammonium acetate in DDW for phase A and 100% methanol for phase B. The gradient profile was: 0–1.00 minutes, 2% B to 100% B; 1.00–30.00 minutes, 100% B; 30.00–37.00 minutes, 2% B; 37.01–40.00 minutes. The flow rate was 0.7 ml/minute, the column temperature was set at 40°C, and the injection volume was 10 µl. Full scan mass spectral data was collected in a *m/z* range of 80 to 1,000 with a scan rate of 1 scan per second.

Green synthesis of Sc-AgNPs

Sc-CE was used in the synthesis of Sc-AgNPs which was modified by Singh and Navneet (2021). The process was prepared in the Laboratory of Pharmacology, Faculty of Veterinary Medicine, Kasetsart University, Thailand. Ninety milliliters of 1 mM $AgNO_3$ and 10 ml of 10% (*w/v*) Sc-CE were mixed by adding Sc-CE slowly, drop by drop, with continuous stirring. The hue of the colloidal solution was steadily turned from translucent to golden-brown color, which indicates the synthesis of Sc-AgNPs. The golden-brown solution was incubated in a dark chamber for 24 hours. Then, the biosynthesized was centrifuged for 20 minutes at 10,000 rpm. The supernatant was discarded. The settled particles were cleaned twice with double-distilled water (ddH_2O) and centrifuged for 5 minutes at 10,000 rpm. Following the cleaning by ddH_2O, ethanol was added to wash the settled particles of Sc-AgNPs before drying under the oven at 55°C (Singh and Navneet, 2021). The Sc-AgNPs powder was kept at 4°C until used.

Characterization of Sc-AgNPs

UV-visible spectroscopic measurements

UV−vis spectrophotometer UV5800 (METASH, USA) was used to record the reduction of Sc-AgNPs in the range of 300 to 550 nm with a 1 nm resolution.

Particle size, Polydispersity Index (PDI), and Zeta(ζ)-Potential Measurements

Characteristic assessments of Sc-AgNPs were performed by the National Nanotechnology Center (NANOTEC, Bangkok, Thailand). Sc-AgNPs powder was dissolved and diluted with ddH_2O to obtain a well-dispersed suspension before use. Then the average hydrodynamic particle size distribution, PDI, and Zeta(ζ)-potential of the Sc-AgNPs solution were measured using a Zetasizer nanoZS (Malvern Instruments, Malvern, U.K.) by dynamic light scattering (DLS) technique. The size measurements were carried out at 25°C, adjusting the light scattering angle at 90°. The surface charge (ζ -potential) of the Sc-AgNPs was measured using an electrophoretic cell under an electric field (Hemlata *et al.*, 2020).

Scanning electron microscope (SEM) and energy-dispersive X-ray analysis (EDAX) of Sc-AgNPs

SEM integrated with EDAX was performed to examine the surface morphology, size, and atomic content of metals in biosynthesized Sc-AgNPs. This analysis was conducted at the Scientific Equipment and Research Division of Kasetsart University, Thailand. The surface morphology of the Sc-AgNPs was measured using an SEM SU8020 (Hitachi, Japan) at a magnification of 100,000× and 200,000×, respectively. The samples were fixed on the tubular platinum stub with double-sided tape. The stub-supported samples were coated with carbon. Finally, the carbon-coated samples were placed under the microscope to observe the morphology (Hemlata *et al.*, 2020).

Microbial strains

The microbial strains used in this study were approved by the Institutional Biosafety Committee, Faculty of Veterinary Medicine, Kasetsart University (IBC-66-05). The gram-positive *Staphylococcus aureus* (ATCC25923) and gram-negative *Pseudomonas aeruginosa* (ATCC27853) were obtained from Armed Forces Research Institute of Medical Sciences.

Three bacterial and two yeast strains were obtained from the Kasetsart University Veterinary Teaching Hospital and identified species by Matrix-assisted laser desorption/ionization-time-of-flight mass spectrometry (JEOL SpiralTOFTM, USA) from the Department of Microbiology and Immunology, Faculty of Veterinary Medicine, Kasetsart University. *Staphylococcus aureus*, *Staphylococcus pseudintermedius*, *P. aeruginosa*, *Malassezia pachydermatis*, and *Candida albicans* were stocked in appropriate conditions.

Antimicrobial activity studies

The *in vitro* antimicrobial susceptibility profiles of Sc-CE and Sc-AgNPs against microbial strains were determined using the assessment of drug sensitivity using the disc diffusion method, agar well diffusion method, assessment of minimum inhibitory concentration (MIC), minimum bactericidal concentration (MBC), minimum fungicidal concentration (MFC), and Time-kill curve Assay observing the guidelines of the Clinical and Laboratory Standards Institute (CLSI, 2020). All experiments were performed at the Laboratory of Pharmacology, Faculty of Veterinary Medicine, Kasetsart University, Thailand.

Assessment of Drug Sensitivity Using Disc Diffusion Method

In the agar disc diffusion test (Kirby-Bauer method) the suspension of a microorganism in saline to the density of a McFarland 0.5 turbidity standard or an absorbance reading of 0.08 to 0.1 at 625 nm (Biologicals, 2014), approximately corresponding to 1 × 108 CFU/ml, was inoculated uniformly onto the surface of an agar plate

(Bubonja-Šonje, 2020). Antibiotic discs, including Ampicillin (10 µg), Amoxicillin (10 µg), Amoxicillin-clavulanic (AMC) (20 µg/10 µg), Doxycycline (DC) (30 µg), and Erythromycin (EM) (15 µg), were prepared and placed on agar surface and then incubated at 37°C for 12 to 16 hours. The zone of inhibition was measured by vernier calliper and identified as susceptible (S), intermediate (I), or resistant (R) by observing the guidelines of the CLSI.

Antimicrobial activity of Sc-CE and Sc-AgNPs using agar well diffusion method

The antibacterial activity of Sc-CE and Sc-AgNPs was determined using the agar well diffusion method. *Staphylococcus aureus*, *S. pseudintermedius*, and *P. aeruginosa* were prepared as an inoculum suspension then each species was spread uniformly on MHA using a sterile loop. A 70 µl of each concentration of the Sc-CE and Sc-AgNPs was added as a triplicate on the plate before incubation at 37°C for 18 to 24 hours. The zone of inhibition of each test sample was measured by vernier calliper.

Assessment of MIC of antibiotic drug using epsilometer test (*E*-test)

E-test, a quantitative technique for determining the antimicrobial susceptibility for MIC determinations in microbiology laboratories around the world, consists of a plastic strip with a continuous gradient of antibiotics immobilized on one side (Citron *et al.*, 1991). Selected pathogens were prepared the same as agar disc diffusion and disc diffusion method. The strips of AMC, DC, and EM were applied in a radial pattern, with one strip applied to each plate. Inoculation of the plates was performed at 37°C for 18 to 24 hours. After incubation, an elliptical inhibition zone was seen around the strip. The MIC value was read from the scale at the intersection of the zone with the *E*-test strip. MIC breakpoints for defining interpretive categories as published by the CLSI.

Determination of MIC

The procedure involves preparing two-fold dilutions of the antimicrobial agent in a liquid growth medium dispensed in tubes containing a minimum volume of 2 ml (macrodilution technique) or with smaller volumes using a 96-well microtitration plate (microdilution technique) (Balouiri *et al.*, 2016). Selected bacterial and yeast strains were prepared according to CLSI guidelines, USA. Sc-CE and Sc-AgNPs were prepared with broth media in 10 concentrations of two-fold dilution. The 100 µl of each concentration was added in each well of 96-well plate microdilution and added on with 100 µl of broth-pathogen except negative control. The incubation time of bacterial strains, *C. albicans*, and *M. pachydermatis* was 18 to 24, 48, and 72 hours, respectively. After inoculation, the MIC was shown as a transparent well of the lowest concentration.

Determination of MBC and MFC

The determination of MBC or MFC, also known as the minimum lethal concentration, was the most common estimation of bactericidal or fungicidal activity. The bactericidal endpoint has been subjectively defined as the lowest concentration, at which 99.9% of the final inoculum is killed. The determination of MBC was performed after broth microdilution by sub-culturing a sample from wells, yielding a negative microbial growth after incubation on the surface of the MHA plate with a sterile loop (Barry *et al.*, 1999). The MFC was also defined as the lowest concentration of the drug that yields a 98% to 99.9% killing effect as compared to the initial inoculum. The determination of MFC was performed after broth microdilution by incubating a sample from wells mixed with 500 µl of broth in Eppendorf at 30°C for 72 hours. The turbidity at the bottom of Eppendorf was shown as a growth of yeast (Arikan, 2007).

Determination of the optimal time using time-kill curve analysis

Time-kill curve analyses were performed by culturing three bacterial strains in a broth culture medium and using four tubes containing a bacterial suspension of 5×10^5 CFU/ml. The first, second, and third tubes contain the molecule, or the extract tested usually at final concentrations of 1 × MIC, 2 × MIC, and 4 × MIC. The fourth one was considered as the growth control. The incubation was done under suitable conditions for varied time intervals (0, 1, 2, 4, 6, 8, 12, and 24 hours) (Pfaller *et al.*, 2004; Konaté *et al.*, 2012). Then, the number of viable cells was calculated relative to the growth control by determining the number of living cells (CFU/ml) of each sample using the agar plate count method.

Determination of acaricidal activity

The MIC level results of Sc-CE and Sc-AgNPs were prepared in concentrations of 1 × MIC, 2 × MIC, and 4 × MIC. Then each group undergoes testing (Sc-CE and Sc-AgNPs) at three different concentrations, determined based on microorganism experimentation outcomes to identify the MIC. The microbial growth test employs flumethrin (6% Bayticol E.C., Bayer, Germany) at a concentration of 40 ppm (mg/l), with distilled water serving as the positive and negative controls, respectively. The experimental procedure will be conducted in triplicate for enhanced accuracy and reliability in the Laboratory of Pharmacology, Faculty of Veterinary Medicine, Kasetsart University, Thailand.

Flea adult contact test

Flea specimens were gathered and identified by the Department of Parasitology, Faculty of Veterinary Medicine, Kasetsart University. Flea was examined species with microscopic examination and characteristics rapidly collected from stray cats in Tanot Temple, Nonthaburi Province. The assay was used as a primary screen to evaluate the contact insecticidal potential of a test compound or extract modified from Weber *et al.* (2019). The two groups of test substances were prepared within a glass vial. Subsequently, the incubation period is initiated, allowing the test substance to uniformly coat the surface of the vial adequately. Once the coating was achieved, the designated punch for testing was introduced to establish contact with the test substance covering the vial's surface. Flea viability was assessed visually by monitoring their movements in comparison to the negative control group. The count of deceased fleas was recorded at intervals of 30 minutes, 1, 2, 4, 6, and 24 hours for subsequent rate calculation, utilizing the following equation for percentage of mortality rate determination: %Mortality = Number of dead flea/Number of initial flea × 100.

Determination of cytotoxicity effect on CPDF using cell viability assay

Fibroblasts have been used as a non-invasive model to study the molecular mechanisms of skin response after exposure to oxidative stress, antioxidants (Pomari *et al.*, 2013), interleukin 1β (Kitanaka *et al.*, 2019), and to unravel their role in the development of atopic dermatitis (Savinko *et al.*, 2012; Berroth *et al.*, 2013; He *et al.*, 2020). This experiment was provided by the Animal Cell Bank, Faculty of Veterinary Medicine, Kasetsart University, Thailand.

Sc-CE and Sc-AgNPs were prepared in DMSO encompassing a total of nine concentrations. The Sc-CE concentrations ranged from 0.625 to 10 mg/ml, while the Sc-AgNPs were utilized at concentrations ranging from 0.005 to 0.5 mg/ml. The 5% DMSO and 0.1% DMSO were used as the positive and negative controls, respectively.

Cell culture

The CPDF was used in this study. It was previously isolated from dogs at Kasetsart University Animal Cell Bank, Faculty of Veterinary Medicine, Kasetsart University. CPDF was maintained in 79% of DMEM, 10% of FBS, and 1% of 100 U/ml penicillin and 100 μg/ml streptomycin. Cells were maintained in humidified air with 5% CO_2 at 37°C. Cells were grown to approximately 70% to 90% confluence and serum-free DMEM was used for cell treatment (Colitti *et al.*, 2023).

Cell viability using MTT assay

Cell viability was evaluated by the MTT colorimetric technique with slight modification (Mosmann, 1983). CPDF (4,500 cells/well) were seeded in a 96-well plate and allowed to grow for 24 hours. They were then treated at various concentrations for 24, 48, and 72 hours. Subsequently, CPDF was incubated with 10 μl of an MTT solution (Sigma, St. Louis, MO) for 4 hours. After the incubation with MTT solution, 100 μl of solubilization solution was added to dissolve water-insoluble purple formazan crystals and the plate was incubated overnight at 37°C in 5% CO_2.

The reduction of MTT in the experiment was assessed through absorbance measurements at a wavelength of 570 nm using Synergy H1 hybrid multi-mode microplate reader (BioTek, Winooski, VT) (Huang *et al.*, 2001). The experiment was conducted in triplicate and obtained values were then employed to calculate the percentage of living cells utilizing the provided equation: % Cell Viability = (OD treated cells – OD blank/OD control cells – OD blank) × 100.

Statistical analysis

All experiments were conducted in triplicate, and the outcomes were expressed as mean ± standard deviation (mean ± SD). All experimental data were analyzed by using GraphPad Prism version 10.1.0. Statistical significance was acknowledged at a significance level of $p < 0.05$.

Ethical approval

The experimental procedure for Acaricidal Activity was performed according to The Guidelines for Animal Experiments and approved by the Animal Ethics Research Committee of the Faculty of Veterinary Medicine, Kasetsart University, Thailand (ACKU66-VET-014).

Results

Phytochemical analysis

The Sc-CE was subjected to comprehensive analysis, revealing a total of 1,679 compounds in positive mode and 1,725 compounds in negative mode which related from the database. However, only 449 and 444 compounds were definitively identified, respectively. Among the substances analyzed, it was observed that the extract contains compounds with diverse properties, including antibiotics, insecticides, antioxidants, antineoplastics, disinfectants, pesticides, antidiabetics, diuretics, antiulceratives, and promoting wound healing, as shown in Table 1.

Furthermore, the analysis highlighted two noteworthy compounds, myricetin and phloretin as illustrated in Figure 1A and B, respectively. These compounds contribute to the diverse range of beneficial properties found in the leaf extract.

Characterizations of Sc-AgNPs

The synthesis of silver nanoparticles utilizing methanol leaf extract was accomplished through the plant-mediated synthesis or green synthesis method. The solution underwent a color transformation from pale green to reddish-brown within 4 hours, indicative of the reduction of Ag+ to Ag0 nanoparticles as shown in Figure 2A. The absorbance of this synthesis solution was measured at 300 to 550 nm. The maximum absorbance showed a peak at 420 nm (Fig. 2B). This reaction indicated the biosynthesis of Sc-AgNPs.

The DLS technique was employed to measure the hydrodynamic particle size distribution, PDI, and surface charge (ζ-potential) of the biosynthesized Sc-AgNPs as detailed in Table 2 and Figure 3A. The average size of the synthesized Sc-AgNPs was approximately 274.6 nm with a low PDI of 0.3, and the ζ-potential was −18.2 mV.

The energy elemental analysis was detected as shown in Figure 3B and Table 2, revealing a discernible peak at 3 keV, indicating the composition of the tested

Table 1. Phytochemical analysis.

Compound name	Formula	Note
3,4,5-Trimethacarb	$C_{11}H_{15}NO_2$	Pesticide, Chinese pesticide, Herbicide
Acequinocyl (AKD-2033X)	$C_{24}H_{32}O_4$	Pesticide
Aldimorph	$C_{18}H_{37}NO$	Pesticide, Fungicide
Ambicromil	$C_{17}H_{12}O_8$	Antihistamine
Amidothioate	$C_{10}H_{15}ClNO_2PS_2$	Pesticide
Aspirin (Acetylsalicylic acid)	$C_9 H_8O_4$	Analgesic, Anti-inflammatory, Antipyretic
Benfuracarb	$C_{20}H_{30}N_2O_5S$	Insecticides
Bisbendazole	$C_{28}H_2 N_6S_4$	Anthelmintic
Butopyronoxyl	$C_{12}H_{18}O_4$	Pesticide
Carbofuranphenol-3-keto	$C_{10}H_{10}O_3$	Pesticide
Clofop-isobutyl	$C_{19}H_{21}ClO_4$	Pesticide, Herbicide
Codlemone	$C_{12}H_{22}O$	Pesticide
Cyfluthrin (II)	$C_{22}H_{18}C_{12}FNO_3$	Insecticides
Desaspidin	$C_{24}H_{30}O_8$	Anthelmintic
Dicyclopentadiene	$C_{10}H_{12}$	Fungicide
Dofamium	$C_{25}H_{44}N_3O_2$	Disinfectant
Empenthrin	$C_{18}H_{26}O_2$	Insecticides
Enocitabine	$C_{31}H_{55}N_3O_6$	Antineoplastic
Enoxolone	$C_{30}H_{46}O_4$	Antiulcerative
Ethyl4-hydroxybenzoate (Ethylparaben)	$C_9H_{10}O_3$	Antiseptic, Antifungal
Febuprol	$C_{13}H_{20}O_3$	Antineoplastic
Ferimzone	$C_{15}H_{18}N_4$	Pesticide
Fluridone	$C_{19}H_{14}F_3NO$	Pesticide, Chinese pesticide, Herbicide
Gamolenic acid	$C_{18}H_{30}O_2$	Anticholesteremic
Gliflumide	$C_{25}H_{29}FN_4O_4S$	Antidiabetic
Hexylresorcinol	$C_{12}H_{18}O_2$	Antiseptic
Lactofen	$C_{19}H_{15}ClF_3NO_7$	Pesticide
Linalool	$C_{10}H_{18}O$	Insecticides
Madecassic acid	$C_{30}H_{48}O_6$	Wound therapeutic
Maduramycin (Maduramicin)	$C_{47}H_{80}O_{17}$	Antibiotic
Mercurophylline	$C_{14}H_{25}HgNO_5$	Diuretic
Methoprene	$C_{19}H_{34}O_3$	Insecticides
Methyl4-hydroxybenzoate (Methylparaben)	$C_8H_8O_3$	Antibacterial, Antifungal
Mitoxantrone	$C_{22}H_{28}N_4O_6$	Antineoplastic
Myricetin	$C_{15}H_{10}O_8$	Antioxidant
Netilmicin	$C_{12}H_{41}N_5O_7$	Antibiotic
Octenidine	$C_{36}H_{62}N_4$	Antiseptic
Palmitic acid glycerol ester	$C_{19}H_{38}O_4$	Fatty acid
Phloretin	$C_{15}H_{14}O_5$	Flavonoid, Antioxidant
Plafibride	$C_{16}H_{22}ClN_3O_4$	Anticholesteremic
Plaunotol	$C_{20}H_{34}O_2$	Antiulcerative
Pyriminobac-mecthyl	$C_{17}H_{19}N_3O_6$	Pesticide

(Continued)

Compound name	Formula	Note
Quinacetol	$C_{11}H_9NO_2$	Pesticide
Quisultidine	$C_{21}H_{25}N_3O_2S_2$	Antiulcerative
Rosaprostol	$C_{18}H_{35}O_3$	Antiulcerative
Rosaramicin	$C_{31}H_{51}NO_9$	Antibiotic
Sulprofos-sulfone-oxon	$C_{12}H_{19}O_5PS_2$	Pesticide
Teniposide	$C_{32}H_{32}O_{13}S$	Antineoplastic
Tocopherol (vitamin E)	$C_{29}H_{50}O_2$	Vitamin
Triflumuron	$C_{15}H_{10}ClF_3N_2O_3$	Insecticides
Trimethoprim-d9	$C_{14}H_9D_9N_4O_3$	Antibiotic, Sulfonamide

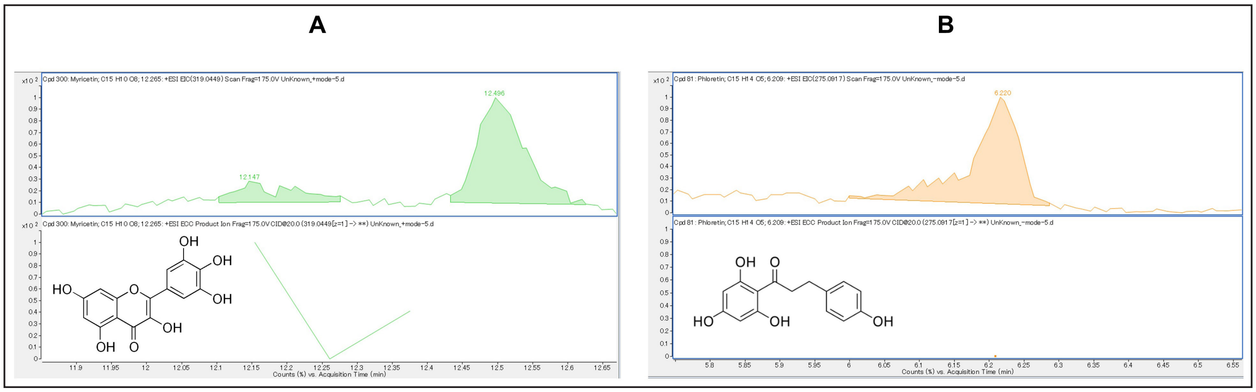

Fig. 1. Chromatogram: (A) myricetin; (B) phloretin.

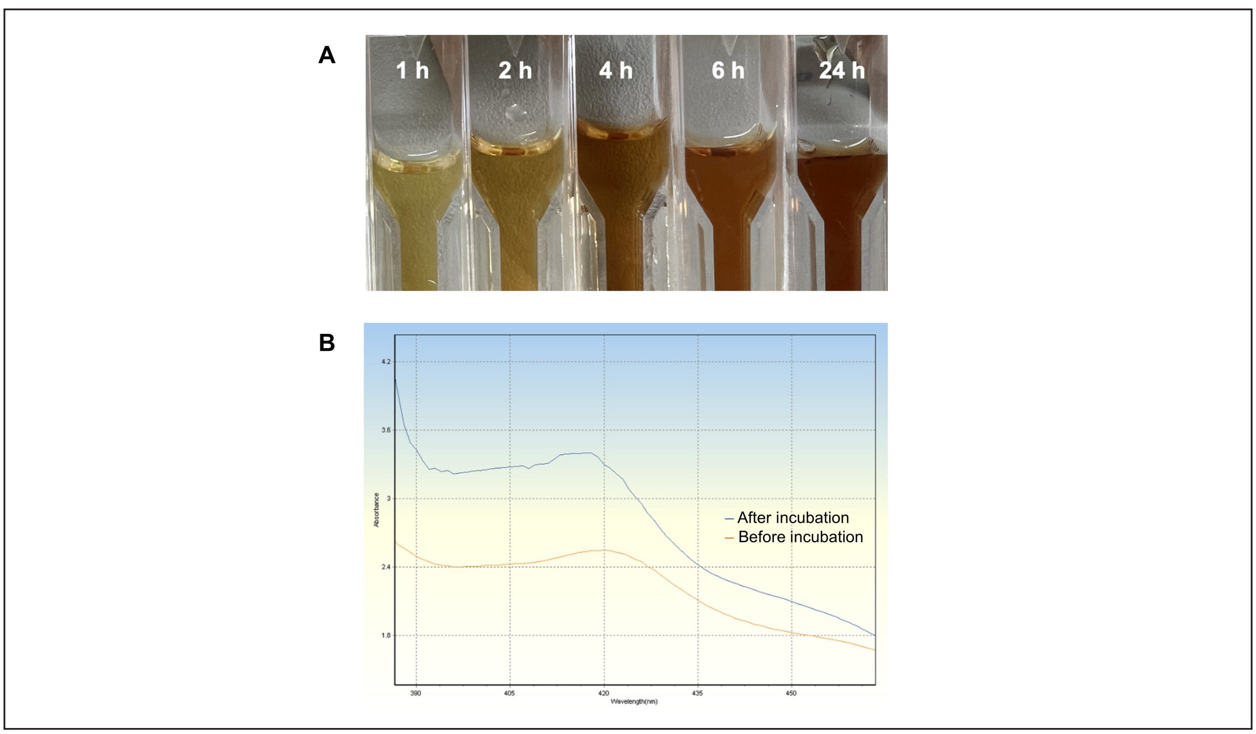

Fig. 2. Silver nanoparticles formation: (A) the colour transformation of biosynthesized silver nanoparticle solution; (B) UV-visible spectroscopic measurement.

Table 2. Physical characterization using DLS technique.

Size (nm)	PDI	Zeta-potential (mV)
274.6	0.3	−18.2
Element	**Weight (%)**	**Atomic mass (%)**
Carbon (C)	66.51	84.27
Oxygen (O)	11.99	11.41
Chlorine (Cl)	4.47	1.92
Silver (Ag)	17.03	2.40

Data are presented as mean of three replications (n = 3). PDI, polydispersity index.

that *S. aureus*, *S. pseudintermedius*, and *P. aeruginosa* exhibited resistance (R) to ampicillin, amoxicillin, and AMC, with *S. pseudintermedius* demonstrating resistance to all three antibiotics. In addition, *P. aeruginosa* did not exhibit an inhibition zone against ampicillin and amoxicillin. Furthermore, *P. aeruginosa* showed resistance to ampicillin, amoxicillin, and AMC. In contrast, susceptibility testing against DC and EM revealed that *S. aureus* was susceptible (S) to both antibiotics, while *S. pseudintermedius* exhibited intermediate sensitivity (I) to DC and EM, displaying resistance without creating a zone of inhibition.

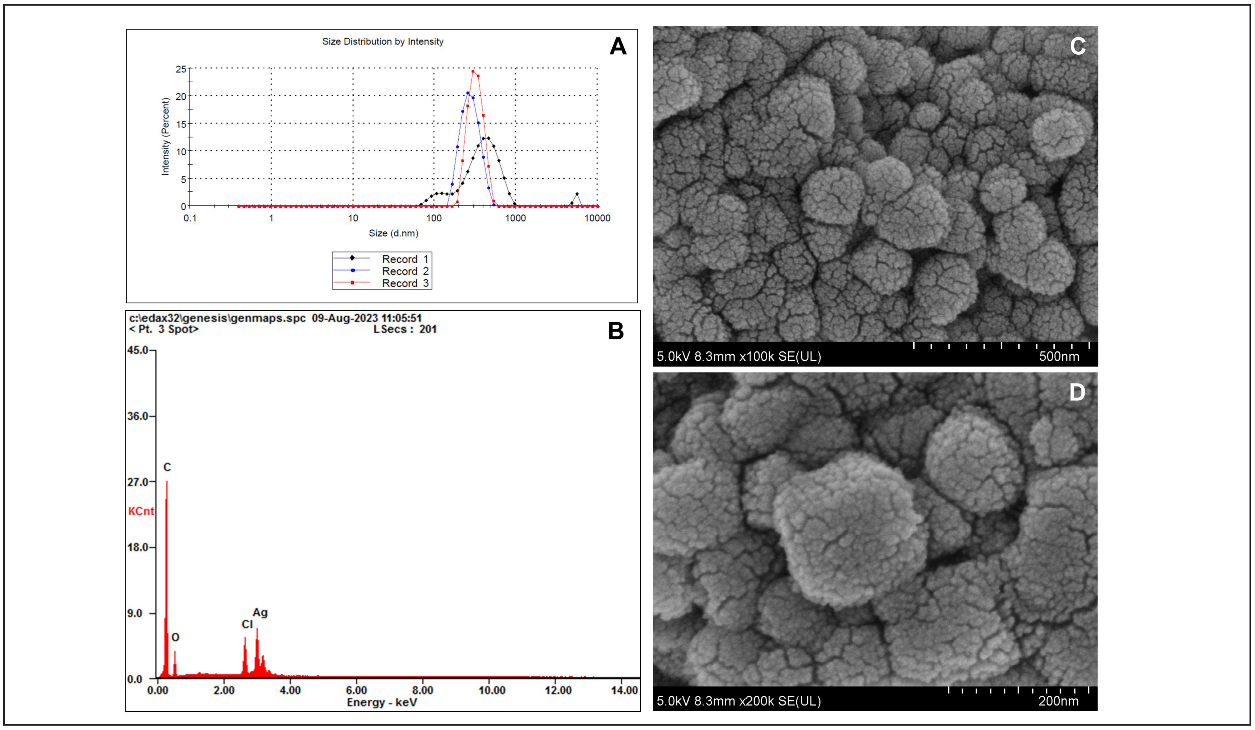

Fig. 3. Physical characterization analysis using (A) DLS technique and electron microscopy assessment: (B) EDX spectra of Sc-AgNPs; (C) SEM analysis 100,000× magnification; (D) SEM analysis 200,000× magnification.

substances. Ag nanoparticles were detected, along with the presence of carbon, oxygen, and chlorine.

The morphology of the green-synthesized Sc-AgNPs was examined using SEM. The analysis revealed polymorphic shapes, with some particles displaying irregular granulation, ellipsoidal structures, and considerable aggregation. The size of Sc-AgNPs ranged from 50 to 200 nm, as shown in Figure 3C and D at a magnification of 100,000× and 200,000×, respectively.

Antimicrobial assays

Assessment of Drug Sensitivity Using Agar Disc Diffusion Method

The susceptibility testing for five antibiotics, ampicillin, amoxicillin, AMC, DC, and EM, was summarized as shown in Table 3. The analysis revealed

Determination of clear zone of inhibition using agar well diffusion method

The effect of Sc-CE and Sc-AgNPs showed inhibited bacteria, as presented in the inhibition clear zone in Table 4. Sc-CE and Sc-AgNPs were a trend to increase the inhibition clear zone of *S. aureus*, *S. pseudintermedius*, and *P. aeruginosa* with increased concentrations. However, Sc-AgNPs were highly effective against pathogens when compared with Sc-CE. Low concentrations of Sc-AgNPs than Sc-CE 10 times also presented the inhibition clear zone. Furthermore, the effect of Sc-AgNPs also inhibited gram-negative bacteria, which was greater than that of gram-positive bacteria.

Table 3. Inhibition zone of antibiotic drug.

Antibiotics	Disk content	Zone of inhibition (mm)					
		S. aureus		*S. pseudintermedius*		*P. aeruginosa*	
Ampicillin	10 µg	20.70 ± 0.26	R	0	R	0	R
Amoxicillin	10 µg	14.17 ± 1.05	R	0	R	0	R
Amoxicillin-clavulanate	20 µg/10 µg	17.83 ± 0.15	R	11.9 ± 0.75	R	0	R
DC	30 µg	26.90 ± 1.10	S	15.2 ± 0.52	I	19.45 ± 0.30	R
EM	15 µg	27.93 ± 0.17	S	0	R	19.15 ± 1.00	R

Interpretive categories and zone diameter breakpoints were interpreted from M100, CLSI, 2020. Data are presented as mean ± SD of three replications (n = 3). S, susceptible; I, intermediate; R, resistant.

Table 4. Inhibition zone of Sc-CE and biosynthesized silver nanoparticles.

Sample	Concentration (mg/ml)	Zone of inhibition (mm)				
		ATCC25923	ATCC27853	*S. aureus*	*S. pseudintermedius*	*P. aeruginosa*
Sc-CE	50	10.80 ± 1.21	14.80 ± 1.04	15.09 ± 0.07	12.69 ± 0.30	19.51 ± 0.23
	40	9.30 ± 0.00	14.50 ± 1.04	14.11 ± 0.16	12.15 ± 0.13	18.34 ± 0.35
	30	7.77 ± 0.25	13.40 ± 0.90	13.08 ± 0.22	11.13 ± 0.01	17.58 ± 0.73
	20	7.20 ± 0.52	12.73 ± 0.81	11.69 ± 0.04	10.01 ± 0.13	16.05 ± 0.42
	10	ND	11.63 ± 0.58	10.66 ± 0.15	ND	14.86 ± 0.34
Sc-AgNPs	1	11.40 ± 0.26	11.03 ± 0.68	9.85 ± 0.35	11.1 ± 0.20	11.75 ± 0.35
	0.5	9.93 ± 0.15	9.70 ± 0.26	7.95 ± 0.25	9.4 ± 0.10	10.4 ± 0.00
	0.4	9.33 ± 0.55	9.07 ± 0.15	7.2 ± 0.40	8.95 ± 0.15	8.7 ± 0.20
	0.2	8.13 ± 0.15	8.03 ± 0.12	ND	7.45 ± 0.05	7.65 ± 0.05
	0.1	7.00 ± 0.17	6.93 ± 0.06	ND	ND	ND
DMSO	1%	ND	ND	ND	ND	ND

Data are presented as mean ± SD of three replications (n = 3). *S. aureus* (ATCC25923); *P. aeruginosa* (ATCC27853). ND = not detected

Determination of MIC of antibiotic using *E*-test

Utilizing the *E*-test method to determine the MIC of antibiotics as shown in Table 5, the results revealed resistance (R) of *S. pseudintermedius* and *P. aeruginosa* to AMC, DC, and EM. Specifically, neither *S. pseudintermedius* nor *P. aeruginosa* exhibited inhibitory zones against DC and EM. Notably, *P. aeruginosa* did not demonstrate an inhibitory zone against any of the three antibiotics. In contrast, *S. aureus* exhibited susceptibility (S) to all three antibiotics.

Determination of MIC, MBC, and MFC

Antimicrobial activity was assessed through the determination of MIC, as presented in Table 6. In comparing the efficacy of inhibiting microbial growth, Sc-AgNPs demonstrated superior performance by utilizing concentrations lower than those required by Sc-CE. Notably, the Sc-AgNPs outperformed the Sc-CE in terms of efficacy.

Time-kill curve assay analysis

The investigation aimed to determine the optimal duration of action for both Sc-CE and Sc-AgNPs against three bacterial strains: *S. aureus* (Fig. 4A and B), *S. pseudintermedius* (Fig. 4C and D), and *P. aeruginosa* (Fig. 4E and F). Over varying time intervals, the test substances exhibited efficacy in inhibiting or killing microorganisms in a concentration-dependent and time-dependent manner. Specifically, higher concentrations of the test substances (4 × MIC) demonstrated greater potency in inhibiting or killing microorganisms compared to lower concentrations (1 × MIC). Moreover, extending the duration of exposure to both Sc-CE and Sc-AgNPs substantially reduced microbial growth. It is noteworthy that Sc-AgNPs exhibited a highly significant reduction in microbial counts during the 8 to 12-hour incubation timeframe.

Assessment of in vitro acaricidal activity using flea adult contact test

All adult fleas were determined the species belong to the Department of Parasitology as *C. felis*, which belonged to the family Pulicidae. These flea's anatomical structures comprised three principal parts: (1) the head, (2) the thorax, and (3) the abdomen. The thorax houses three pairs of legs, with the third pair distinguished as

Table 5. MIC of antibiotic strap (*E*-test).

Pathogen	Antibiotic strap *E*-test (µg/ml)					
	AMC		DC		EM	
S. aureus	1	S	1	S	2	S
S. pseudintermedius	64	R	>256	R	>256	R
P. aeruginosa	>256	R	>256	R	>256	R

Interpretive categories and zone diameter breakpoints were interpreted from M100, CLSI, 2020. Data are presented as the minimum concentration of three replications (n = 3). AMC, amoxycillin clavulanic acid; DC, doxycycline; EM, erythromycin; R, resistant; S, susceptible.

Table 6. MIC, MBC, and MFC of Sc-CE and Sc-AgNPs against pathogens.

Pathogen	Sc-CE (mg/ml)		Sc-AgNPs (mg/ml)	
	MIC	MBC or MFC	MIC	MBC or MFC
S. aureus (ATCC25923)	50	100	0.25	1
P. aeruginosa (ATCC27853)	25	100	0.25	0.5
S. aureus	6.25	25	0.25	1
S. pseudintermedius	3.125	6.25	0.25	1
P. aeruginosa	12.5	50	0.05	0.5
M. pachydermatis	6.25	12.5	0.125	0.125
C. albicans	25	100	0.008	0.016

Data are presented as the minimum concentration of three replications (n = 3).

jumping legs, surpassing the length of the other two pairs (Fig. 5A).

The cumulative mortality rate of *C. felis* was summarized in Figure 5B and C. The evaluation of all groups of substances involving the exposure of fleas to Sc-CE and Sc-AgNPs showed increased mortality with progressively slower movement until complete cessation from 30 minutes to 1, 2, 4, 6, and 24 hours. Consequently, all groups of Sc-CE and Sc-AgNPs demonstrated concentration-dependent and time-dependent responses against external parasites, specifically fleas. Upon administering, specifically 100 mg/ml of Sc-CE and 1 mg/ml of Sc-AgNPs resulted in cumulative mortality rate of 93.3% and 90.0% within 24 hours, respectively.

Determination of CPDF using cell viability assay

Characterization of CPDF was shown in Figure 6A and exhibited a fusiform (spindle-shaped) morphology with spreading growth resembling branching. The assessment of the cell viability of CPDF following exposure to Sc-CE and Sc-AgNPs at 24, 48, and 72 hours was exhibited in Figure 6B and C, respectively. In the range of treated concentration, both Sc-CE and Sc-AgNPs reduced the viability of the CPDF in a concentration-dependent manner. After 24 hours of treatment, the Sc-CE at a concentration of 5 to 10 mg/ml reduced CPDF viability to less than 50% of the initial level. However, Sc-AgNPs at a concentration of 0.005 to 0.5 mg/ml did not reduce CPDF viability to below 50% of the initial level after 24, 48, and 72 hours of treatment. The optimal effective concentrations, 0.5 mg/ml for Sc-AGNPs and 2.5 mg/ml for Sc-CE, showed the lowest cytotoxicity in CPDF at 24 hours of treatment.

Discussion

Extraction of plants as leaves can be carried out using various solvents, such as methanol, ethanol, hexane, chloroform, acetone, and water, among others. Previous research has shown that methanol can effectively extract compounds from plant material. Thus, to ensure the extraction of important compounds, the present study opted to use methanol as the extraction solvent. Methanol is a chemical that belongs to the alcohol group and has a hydroxyl group (−OH) that makes it effective in extracting a wide range of plant compounds (Cowan, 1999).

The leaves of *S. cumini* are known to contain flavonoids like myricetin and gallic acid (Gaspar *et al.*, 2020), attributed to various medical properties such as anti-cancer (Zhao *et al.*, 2019), antimicrobial, antiviral (Camero *et al.*, 2018; Zhao *et al.*, 2018), antimalarial, and antioxidant effects, as well as neuroprotective properties (Patel *et al.*, 2018). The leaf extract analysis revealed the presence of myricetin and phloretin, both flavonoid compounds with diverse medical benefits.

Myricetin, a flavonoid compound prevalent in various plant parts, is an essential nutritional component

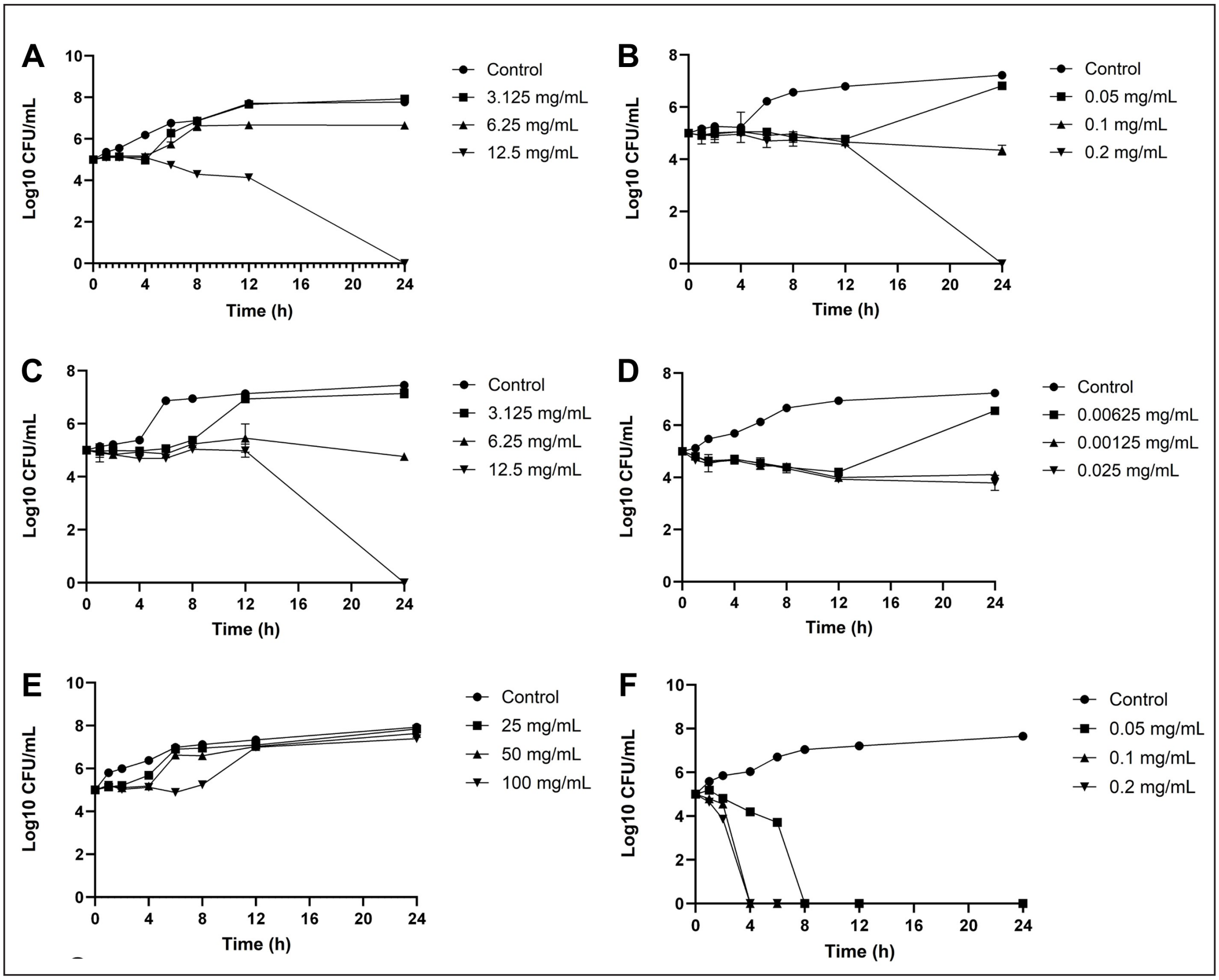

Fig. 4. Time-kill curve assay analysis: *S. aureus* (A) Sc-CE; (B) Sc-AgNPs, *S. pseudintermedius* (C) Sc-CE; (D) Sc-AgNPs, *P. aeruginosa* (E) Sc-CE; (F) Sc-AgNPs.

and well known for its antioxidant properties. It is recognized for its potential to combat cancer, lower elevated blood sugar levels, and alleviate inflammation. Additionally, Myricetin played a significant role in supporting the central nervous system (Semwal *et al.*, 2016). Phloretin, also known as dihydronaringenin or phloretol, belongs to the dihydrochalcone group within the flavonoid category. As a natural polyphenol substance, it is abundantly found in a variety of vegetables and fruits, particularly in the leaves of apple and Manchurian apricot. Medically, phloretin is valued for its diverse therapeutic properties, serving as an antioxidant, antidiabetic agent, anti-inflammatory compound, and anticancer substance. Its applications extend to inhibiting the progression of various cancers (Tuli *et al.*, 2022). A study by Adamczak *et al.* (2019) has explored the antimicrobial effects of medicinal plant extracts and highlighted that the antimicrobial efficacy of Sc-CE may depend on the interaction of various important compounds.

In the synthesis of silver nanoparticles from *S. cumini*, the study of Hemlata *et al.* (2020) focused on their physical properties. The hydrodynamic size, which includes the hydration layer on the surface of AgNPs, was generally larger than the size measured from SEM images. Additionally, the phytochemicals in the leaf extract may contribute to the hydrodynamic size. Nanoparticles with a size below 150 nm and PDI values around 0.3 are suitable for cellular uptake, indicating the effectiveness of lipid-based carriers for drug administration (Batista *et al.*, 2016; Zhao *et al.*, 2019). Zeta potential measurements suggested stability, crucial for expel ability and dispersion of particles (Mariadoss *et al.*, 2019). The higher the negative or positive ζ-potential, the higher the stability, the better the colloidal properties due to electrostatic repulsion, and the higher the dispersity (Mariadoss *et al.*, 2019).

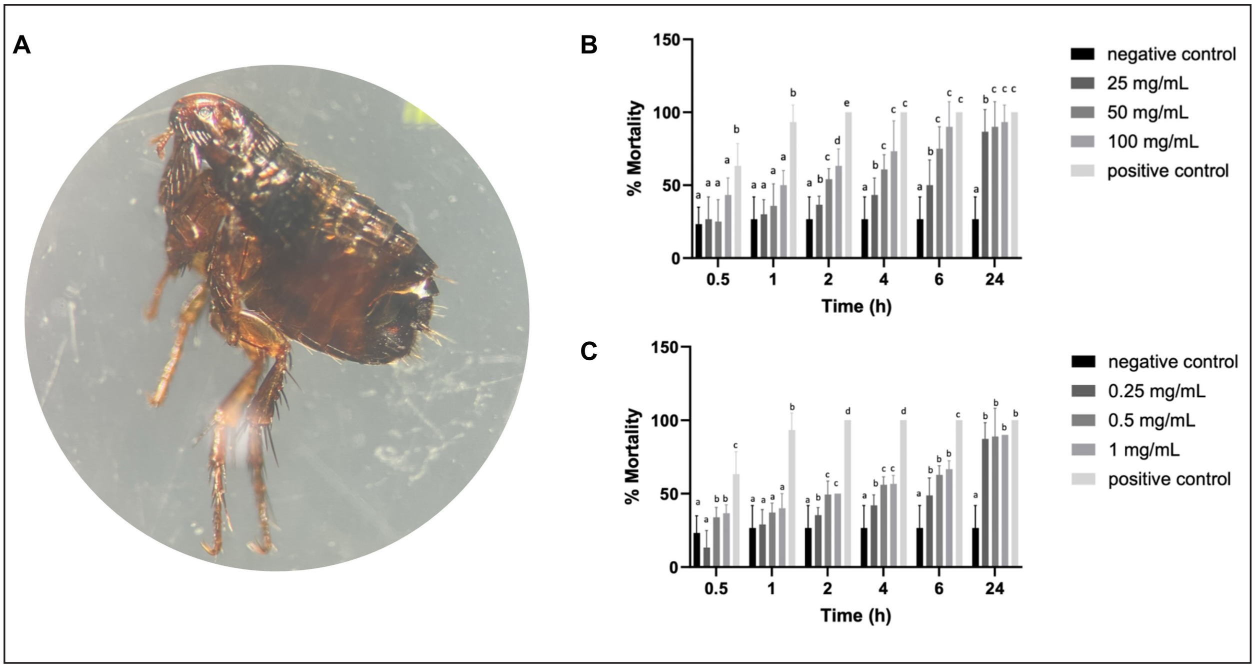

Fig. 5. Assessment of acaricidal activity: (A) *Ctenocephalides felis* under a stereomicroscope (B) Sc-CE; (C) Sc-AgNPs. The bars indicate the average of triplicate (n = 3) and SD. The positive control was flumetrin. The negative control was distilled water. Different letters show significant differences among groups obtained by one-way analysis of variance (ANOVA) multiple comparisons.

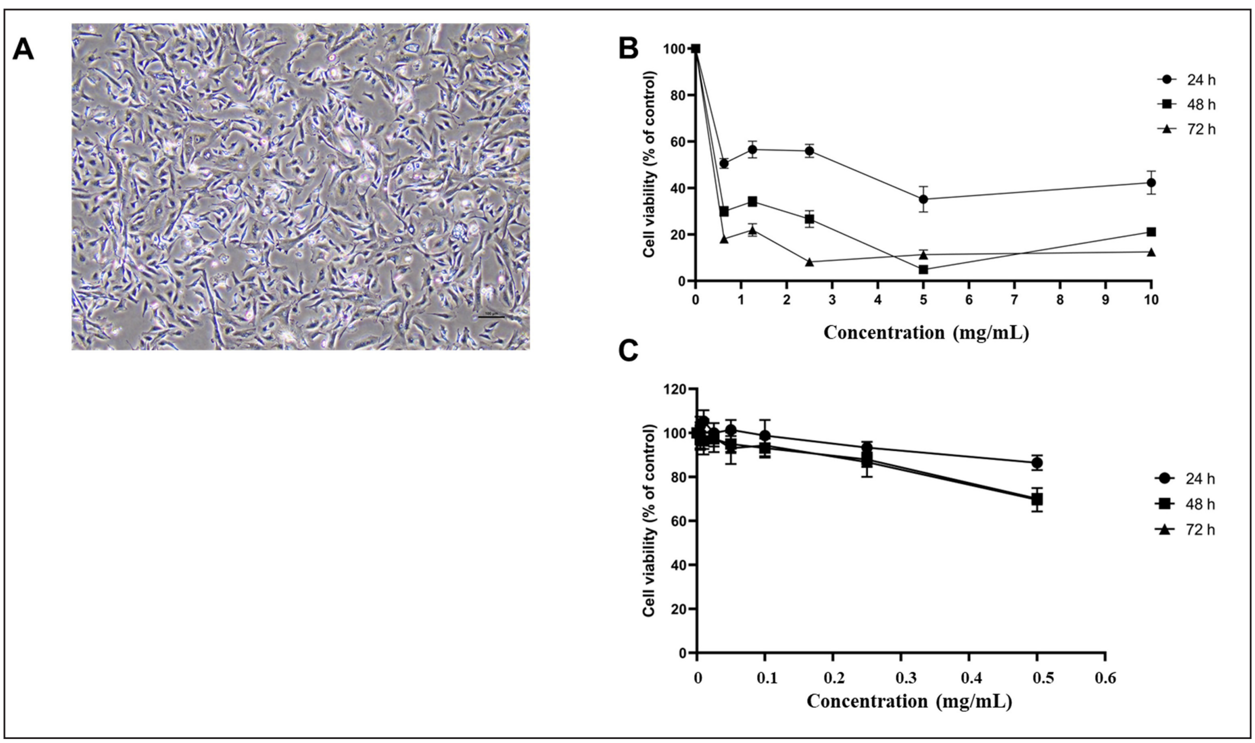

Fig. 6. Cytotoxicity assay: (A) CPDF (B) Sc-CE concentration of 6.25–10 mg/ml; (C) Sc-AgNPs concentration of 0.005–0.5 mg/ml.

The ζ-potential of Sc-AgNPs was negative, suggesting that negatively charged functional groups from the plant extract contribute to the colloidal stability of the AgNPs (Ahn *et al.*, 2019).

The main elements in silver nanoparticles revealed the presence of carbon and oxygen, linked to the organic compounds in the plant extraction, including *S. cumini* leaf extract, found on the surface of the silver nanoparticles synthesized using Sc-CE (Patel *et al.*, 2018). These organic compounds played a pivotal role in the reduction and stabilization reactions during the synthesis of silver nanoparticles with Sc-CE. Meanwhile, Sc-AgNPs were found to be 50–100 times more effective than Sc-CE.

Previous study reported the antimicrobial effects of *S. cumini* including leaves (Mohamed *et al.*, 2013). In the present study, the extraction and nanoparticle synthesis compound from Sc demonstrated antibacterial activity *in vitro* against both gram-positive and gram-negative bacteria, consistent with this previous study. However, the bacteria tested in this study were mostly recognized as antimicrobial-resistant, showing resistant to commonly used antibiotics, such as Ampicillin, Amoxicillin, AMX, DC, and EM, for treating canine skin diseases. Despite this resistance, Sc-CE and Sc-AgNPs exhibited not only bacterial inhibition but also inhibition of yeasts like *C. albicans* and *M. pachydermatis*. Sc-AgNPs were effective at a concentration starting from 0.4 mg/ml against all test bacteria and could decrease the colony of bacteria within 8–12 hours, especially *P. aeruginosa*, at a concentration as low as 0.05 mg/ml. The nanoparticle of Sc-AgNPs likely enhanced the distribution of active compounds through bacterial cells and then interfered with microorganism activities. Generally, microorganisms such as bacteria and yeast are classified as prokaryotes, while external parasites are classified as eukaryotes. Both organisms contain ion channels and proteins in their cell wall that serve as passageways and regulate ions flow in and out of the cell. For instance, the sodium channel specifically controls the movement of sodium ions (Stanneck *et al.*, 2012). This study revealed that some active compounds in Sc-CE and Sc-AgNPs, such as flavonoids, significantly affect the sodium channel of both prokaryote and eukaryote cells. While various reports have mentioned the antibacterial effect of *S. cumini*, the present study also found that Sc-CE and Sc-AgNPs could combat antimicrobial-resistance bacteria and yeast.

Cat fleas such as *C. felis* are the most common ectoparasites found on both domestic cats and dogs globally, and they are frequently found on stray cats and dogs. In this study, flea samples were intentionally gathered from stray animals after ensuring their previous non-exposure to ectoparasite products in their life for Sc-CE and Sc-AgNPs treatments. Many studies have reported the effect of plant extracts on insects, worms, and parasites. In the present study, we also found that Sc-CE and Sc-AgNPs disrupted fleas' cell metabolism, leading to their death within 24 hours. This finding aligns with a previous study by Batista *et al.* (2016), which investigated the impact of oil extracts from pink pepper (*Schinus molle*) leaves and fruits on *C. felis*. Remarkably, Sc-CE and Sc-AgNPs demonstrated significant effectiveness in eliminating fleas, achieving a cumulative death rate exceeding 50% within a short span of 4 to 6 hours. The cumulative mortality rate of fleas increased with both the concentration of Sc-CE and Sc-AgNPs and the duration of exposure. These results suggest that the effectiveness of these substances increased in tandem with the dosage and duration of contact. Sc-CE and Sc-AgNPs may interact with a potential mechanism of action on sodium channels in cells of fleas, like flumethrin, an insecticide that is classified as Type II Pyrethroid. This mechanism involves the modulation of sodium channel activity, leading to prolonged depolarization of nerve cells and disruption of neurotransmitter binding at nerve endings, ultimately causing seizures and death (Stanneck *et al.*, 2012). These reasons might demonstrate the effectiveness of Sc-CE and Sc-AgNPs against ectoparasite in this study.

Current investigations focus on the impact of water extracts on cancer cells (Colitti *et al.*, 2023). Promisingly, these extracts exhibited the ability to inhibit cancer cell growth and induce apoptosis. Importantly, there have not been any reported effects on promoting the growth of normal cells. Thus, in this study to assess the cytotoxicity of the test substances, CPDF served as a suitable surrogate. These cells, resembling the living skin of dogs, provided insights into the response after exposure to the test substances, as outlined by Colitti *et al.* (2023). Notably, the cell viability rate decreased slowly within 24 hours. These results demonstrated that Sc-CE and Sc-AgNPs mediated a concentration and time-dependent increase in cytotoxicity. This finding contradicted the conventional expectation that higher concentrations of substance would not be more toxic and result in decreased cell viability. However, both compounds showed the lowest cytotoxicity in CPDF at 24 hours of treatment. Therefore, they may be suitable for use with less toxicity to CPDF as a topical application for 24 hours of treatment.

Conclusion

In conclusion, the results suggested that Sc-CE, used in the biosynthesis of silver nanoparticles, possesses significant selectivity for antimicrobial, and antiparasitic activities and can display potential and safety for topical applications. This impact on microorganisms was found to be comparable to widely used antibiotics, thereby helping to mitigate the risk of drug resistance development. The synthesis process of silver nanoparticles using medicinal plants was identified as a simple, convenient, economical, and environmentally friendly method. Moreover, utilizing Sc-AgNPs at a concentration at least 50 times lower than that of the Sc-CE retained comparable antimicrobial efficacy and achieved results within 24 hours, offering a strategy to avoid potential toxic effects associated with excessive silver use. Furthermore, both Sc-CE and Sc-AgNPs exhibited concentration-dependent and time-dependent effects. This point was mentioned that increasing the concentration of these solutions and extending the contact time could enhance their efficacy. Although current medical literature lacks clear reports on the toxicity of silver nanoparticles, caution is recommended. Future developments, particularly for external applications on animals, should prioritize safety. Testing on CPDF revealed that the Sc-CE, aside from not inducing dangerous levels of toxicity, actively promoted cell growth at appropriate concentrations. Moreover, the efficient result of Sc-AgNPs in the concentration and time that served probably as bactericidal, there were safe to treat CPDF within 24 hours. It is important to note that limitations exist in the processes for obtaining extracts and silver nanoparticles, particularly concerning the quantities obtained from extraction and synthesis steps. As a result, achieving comparable concentrations of Sc-AgNPs and Sc-CE for testing in various steps may prove challenging in the future.

Acknowledgments

The authors would also like to acknowledge the Central Laboratory, Faculty of Veterinary Medicine, Kasetsart University, for sample preparation and the Department of Microbiology and Immunology, Faculty of Veterinary Medicine, Kasetsart University, and Hokkaido University, for LC/QTOF-MS analysis.

Conflict of interest

The authors declare no conflicts of interest.

Funding

This research funding was supported from Graduate Development Research Grants and Research Potential Development of Faculty of Veterinary Medicine Researcher Grants by the Department of Pharmacology, Faculty of Veterinary Medicine, Kasetsart University and Assis. Prof. Aksorn Saengtienchai, Ph.D.

Author contribution

Conceptualization: Wongstitwilairoong N; Data curation: Wongstitwilairoong N; Formal analysis: Wongstitwilairoong N, Saengtienchai A; Funding acquisition: Saengtienchai A; Investigation: Saengtienchai A; Methodology: Wongstitwilairoong N, Saengtienchai A, Jermnark U, Limsivilai O, Chimnoi W, Juratha J Yohannes YB Ikenaka Y; Project administration: Wongstitwilairoong N, Saengtienchai A; Resources: name; Software: Microsoft Word, Microsoft PowerPoint, GrapdPad Prism ver 10.1.0; Supervision: Saengtienchai A; Validation: Wongstitwilairoong N, Saengtienchai A; Visualization: Wongstitwilairoong N, Saengtienchai A; Writing - original draft: Wongstitwilairoong N; Writing - review & editing: Saengtienchai A.

Data availability

All data supporting the findings of this study are available within the manuscript.

References

Adamczak, A., Ożarowski, M. and Karpiński, T.M. 2019. Antibacterial activity of some flavonoids and organic acids widely distributed in plants. J. Clin. Med. 9(1), 109.

Ahn, E.Y., Jin, H. and Park, Y. 2019. Assessing the antioxidant, cytotoxic, apoptotic and wound healing properties of silver nanoparticles green-synthesized by plant extracts. Mater Sci. Eng. C Mater Biol. Appl. 101, 204–216.

Arikan, S. 2007. Current status of antifungal susceptibility testing methods. Med. Mycol. J. 45(7), 569–587.

Balouiri, M., Sadiki, M. and Ibnsouda, S.K. 2016. Methods for in vitro evaluating antimicrobial activity: a review. J. Pharma. Anal. 6(2), 71–79.

Barry, A.L., Craig, W.A., Nadler, H., Reller, L.B., Sanders, C.C. and Swenson, J.M. 1999. Methods for determining bactericidal activity of antimicrobial agents. Approved guideline. 19, 1–3.

Batista, L.C., Cid, Y.P., De Almeida, A.P., Prudêncio, E.R., Riger, C.J., De Souza, M.A., Coumendouros, K. and Chaves, D.S. 2016. In vitro efficacy of essential oils and extracts of Schinus molle L. against Ctenocephalides felis felis. Parasitology. 143(5), 627–638.

Berroth, A., Kühnl, J., Kurschat, N., Schwarz, A., Stäb, F., Schwarz, T., Wenck, H., Fölster-Holst, R. and Neufang, G. 2013. Role of fibroblasts in the pathogenesis of atopic dermatitis. J. Allergy Clin. Immunol. 131(6), 1547–1554.

Biologicals D. 2014. McFarland standard-for in vitro use only. Canada: Dalynn.

Bubonja-Šonje, M., Knežević, S. and Abram M. 2020. Challenges to antimicrobial susceptibility testing of plantderived polyphenolic compounds. Arh. Hig. Rada Toksikol. 71(4), 300–311.

Camero, C.M., Germanò, M.P., Rapisarda, A., D'Angelo, V., Amira, S., Benchikh, F., Braca, A. and Leo, M.D. 2018. Anti-angiogenic activity of iridoids from Galium tunetanum. Rev. Bras. Farmacogn. 28(3), 374–377.

Citron, D.M., Ostovari, M.I., Karlsson, A. and Goldstein, E.J. 1991. Evaluation of the E test for susceptibility testing of anaerobic bacteria. J. Clin. Microbiol. 29(10), 2197–2203.

CLSI. 2020. Performance standards for antimicrobial susceptibility testing. 30th ed. CLSI supplement M100. Wayne, PA: Clinical and Laboratory Standards Institute.

CLSL. 2020. Performance Standards for Antimicrobial Susceptibility Testing. 30th ed. CLSI supplement M100. Wayne, PA: Clinical and Laboratory Standards Institute.

Colitti, M., Stefanon, B., Sandri, M. and Licastro, D. 2023. Incubation of canine dermal fibroblasts with serum from dogs with atopic dermatitis activates extracellular matrix signalling and represses oxidative phosphorylation. Vet. Res. Commun. 47(1), 247–258.

Cowan, M.M. 1999. Plant products as antimicrobial agents. Clin. Microb. Rev. 12(4), 564–582.

Gaspar, R.S., Silva, S.A.da., Stapleton, J., Fontelles, J.L.de.L., Sousa, H.R., Chagas, V.T., Alsufyani, S., Trostchansky, A., Gibbins, J.M. and Paes, A.M.de.A. 2020. Myricetin, the main flavonoid in *Syzygium cumini* leaf, is a novel inhibitor of platelet thiol isomerases PDI and ERp5. Front. Pharmacol. 10, 1678.

He, S., Wang, L.H., Liu, Y., Li, Y.Q., Chen, H.T., Xu, J.H., Peng, W., Lin, G.W., Wei, P.P., Li, B., Xia, X., Wang, D., Bei, J.X., He, X. and Guo, Z. 2020. Single-cell transcriptome profiling of an adult human cell atlas of 15 major organs. Genome Biol. 21(294), 1–34.

Hemlata, M.P.R., Singh, A.P. and Tejavath, K.K. 2020. Biosynthesis of silver nanoparticles using cucumis prophetarum aqueous leaf extract and their antibacterial and antiproliferative activity against cancer cell lines. ACS Omega 5(10), 5520–5528.

Huang, F.M., Tai, K.W., Hu, C.C. and Chang, Y.C. 2001. Cytotoxic effects of denture base materials on a permanent human oral epithelial cell line and on primary human oral fibroblasts in vitro. Int. J. Prosthodont. 14(5), 439–443.

Kaneria, M. and Chanda, S. 2013. Evaluation of antioxidant and antimicrobial capacity of *Syzygium cumini* L. leaves extracted sequentially in different solvents. J. Food Biochem. 37(2), 168–176.

Kitanaka, N., Nakano, R., Sugiura, K., Kitanaka, T., Namba, S., Konno, T., Nakayama. N. and Sugiya, H. 2019. Interleukin-1beta promotes interleulin-6 expression via ERK1/2 signaling pathway in canine dermal fibroblasts. PLoS One 14(7), 0220262.

Konaté, K., Mavoungou, J.F., Lepengué, A.N., Aworet-Samseny, R.R., Hilou, A., Souza, A., Dicko, M.H. and M'batchi B. 2012. Antibacterial activity against β-lactamase producing Methicillin and Ampicillin-resistants Staphylococcus aureus: fractional inhibitory concentration index (FICI) determination. Ann. Clin. Microbiol. Antimicrob. 11(18), 1–12.

Mariadoss, A.V.A., Ramachandran V., Shalini, V., Agilan, B., Franklin, J.H., Sanjay, K., Alaa, Y.G., Tawfiq, M.A. and Ernest, D. 2019. Green synthesis, characterization and antibacterial activity of silver nanoparticles by Malus domestica and its cytotoxic effect on (MCF-7) cell line. Microb. Pathog. 135, 103609.

Mohamed, A.A., Ali, S.I. and El-Baz, F.K. 2013. Antioxidant and antibacterial activities of crude extracts and essential oils of *Syzygium cumini* leaves. PLoS One 8(4), 60269.

Mosmann, T. 1983. Rapid colorimetric assay for cellular growth and survival: application to proliferation and cytotoxicity assays. J. Immunol. Methods. 65(1-2), 55-63.

Patel, K., Kumar, V., Rahman, M., Verma, A. and Patel, D.K. 2018. New insights into the medicinal importance, physiological functions and bioanalytical aspects of an important bioactive compound of foods 'Hyperin': health benefits of the past, the present, the future. BJBAS 7(1), 31–42.

Pfaller, M., Sheehan, D. and Rex, J. 2004. Determination of fungicidal activities against yeasts and molds: lessons learned from bactericidal testing and the need for standardization. Clin. Microbol. Rev. 17(2), 268–280.

Pomari, E., Stefanon, B. and Colitti, M. 2013. Effect of *Arctium lappa* (burdock) extract on canine dermal fibroblasts. Vet. Immunol. Immunopathol. 156(3–4), 159–166.

Savinko, T., Matikainen, S., Saarialho-Kere, U., Lehto, M., Wang, G., Lehtimäki, S., Karisola, P., Reunala, T., Wolff, H., Lauerma, A. and Alenius, H. 2012. IL-33 and ST2 in atopic dermatitis: expression profiles and modulation by triggering factors. J. Invest. Dermatol. 132(5), 1392–1400.

Semwal, D.K., Semwal, R.B., Combrinck, S. and Viljoen, A. 2016. Myricetin: a dietary molecule with diverse biological activities. Nutrients. 8(2), 90.

Singh, R. and Navneet. 2021. Green synthesis of silver nanoparticles using methanol extract of Ipomoea carnea Jacq. to combat multidrug resistance bacterial pathogens. CRGSC. 4, 100152.

Stanneck, D., Ebbinghaus-Kintscher, U., Schoenhense, E., Kruedewagen, E.M., Turberg, A., Leisewitz, A., Jiritschka, W. and Krieger, K.J. 2012. The synergistic action of imidacloprid and flumethrin and their release kinetics from collars applied for ectoparasite control in dogs and cats. Parasit Vectors. 5(73), 1–18.

Tuli, H.S., Rath, P., Chauhan, A., Ramniwas, S., Vashishth, K., Varol, M., Jaswal, V.S., Haque, S. and Sak, K. 2022. Phloretin, as a potent anticancer compound: from chemistry to cellular interactions. Molecules. 27(24), 8819.

Weber, S.S., Kaminski, K.P., Perret, J.L., Leroy, P., Mazurov, A., Peitsch, M.C., Ivanov, N.V. and Hoeng, J. 2019. Antiparasitic properties of leaf extracts derived from selected Nicotiana species and Nicotiana tabacum varieties. Food Chem. Toxicol. 132, 110660.

WHO. 2017. Prioritization of pathogens to guide discovery, research and development of new antibiotics for drug-resistant bacterial infections, including tuberculosis. World Health Organization. Report No. 9240026436.

Zhao, K., Yuan, Y., Lin, B., Miao, Z., Li, Z., Guo, Q. and Lu, N. 2018. LW-215, a newly synthesized flavonoid, exhibits potent anti-angiogenic activity in vitro and in vivo. Gene. 642, 533–541.

Zhao, L., Yuan, X., Wang, J., Feng, Y., Ji, F., Li, Z. and Bian, J. 2019. A review on flavones targeting serine/threonine protein kinases for potential anticancer drugs. Bioorg. Med. Chem. 27(5), 677–685.